Mechanistic Characterization of the Bifunctional Aminoglycoside-Modifying Enzyme AAC(3)-Ib/AAC(6′)-Ib′ from *Pseudomonas aeruginosa*

Choonkeun Kim, Adriel Villegas-Estrada, Dusan Hesek, and Shahriar Mobashery*

Department of Chemistry and Biochemistry, University of Notre Dame, Notre Dame, Indiana 46556

Received January 18, 2007; Revised Manuscript Received March 7, 2007

ABSTRACT: A recently discovered bifunctional antibiotic-resistance enzyme named AAC(3)-Ib/AAC(6′)-Ib′, from *Pseudomonas aeruginosa*, catalyzes acetylation of aminoglycoside antibiotics. Since both domains are acetyltransferases, each was cloned and purified for mechanistic studies. The AAC(3)-Ib domain appears to be highly specific to fortimicin A and gentamicin as substrates, while the AAC(6′)-Ib′ domain exhibits a broad substrate spectrum. Initial velocity patterns indicate that both domains follow a sequential kinetic mechanism. The use of dead-end and product inhibition and solvent-isotope effect reveals that both domains catalyze their reactions by a steady-state ordered Bi−Bi kinetic mechanism, in which acetyl-CoA is the first substrate that binds to the active site, followed by binding of the aminoglycoside antibiotic. Subsequent to the transfer of the acetyl group, acetylated aminoglycoside is released prior to coenzyme A. The merger of two genes to create a bifunctional enzyme with expanded substrate profile would appear to be a recent trend in evolution of resistance to aminoglycoside antibiotics, of which four examples have been documented in the past few years.

Aminoglycoside-modifying enzymes are the predominant causes of bacterial resistance to aminoglycoside antibiotics. These enzymes are grouped into three families, aminoglycoside phosphotransferases (APHs), aminoglycoside acetyltransferases (AACs), and aminoglycoside nucleotidyltransferases (ANTs). The turnover products of these reactions lack antibacterial activity. Each class performs a specific reaction. Furthermore, several subtypes of each class have been identified with distinct regioselectivities in substrate modification. For example, AAC(3)-Ib is an aminoglycoside acetyltransferase that acetylates the antibiotics at the 3-amino group, and the Ib designation indicates that gentamicin and fortimicin A serve as substrates. The AACs, and other aminoglycoside-modifying enzymes, are typically monofunctional enzymes (*1−3*).

Bifunctional enzymes are generally rare in bacteria. Four genes encoding bifunctional aminoglycoside-resistance enzymes have now been discovered within the past few years. These genes encode enzymes that have been designated as AAC(6′)/APH(2″), ANT(3″)-Ii/AAC(6′)-IId, AAC(3)-Ib/AAC(6′)-Ib′, and AAC(6′)-30/AAC(6′)-Ib′. The mechanism of AAC(6′)/APH(2″) has been studied extensively (*4−8*). We described the properties of ANT(3″)-Ii/AAC(6′)-IId recently (*9*). However, AAC(3)-Ib/AAC(6′)-Ib′ and AAC-(6′)-30/AAC(6′)-Ib′ have not been investigated in enzymological studies.

The gene for the new bifunctional aminoglycoside-modifying enzyme from *Pseudomonas aeruginosa*, designated *aac(3)-Ib/aac(6′)-Ib′*, was described recently (*10*). The nucleotide sequence of the *aac(3)-Ib* portion of the gene is identical to that of the *aac(3)-Ib* gene isolated from *P.*

aeruginosa in 1995 (*1*), except for the deletion of the last 15 nucleotides. This gene segment confers resistance to gentamicin and fortimicin A. The nucleotide sequence of the *aac(6′)-Ib′* portion of the gene is 99% identical to that of the previously described *aac(6′)-Ib′* gene (*11−13*). Harboring of this gene manifests resistance to kanamycin and tobramycin, reduced susceptibility to netilmicin and amikacin, and undiminished susceptibility to gentamicin. The *aac(3)-Ib* and *aac(6′)-Ib′* genes each express as monofunctional enzymes. Only two AAC(3) enzymes, AAC(3)-I (*14*) and AAC(3)-IV (*15*), have been studied for their kinetic mechanisms, both of which follow a random sequential mechanism. This general lack of information on the AAC(3)s is despite their wide distribution among different bacterial genera. The discovery of the bifunctional AAC(3)-Ib/AAC(6′)-Ib′ now adds an intriguing new chapter in the evolution of AACs. We have undertaken a study of this newly discovered bifunctional aminoglycoside-modifying enzyme. We describe herein the kinetic mechanisms of AAC(3)-Ib/AAC(6′)-Ib′ using several analyses including initial velocity pattern, substrate specificity, inhibition pattern, and solvent-isotope effect.

EXPERIMENTAL PROCEDURES

Construction of AAC(3)-Ib/AAC(6′)-Ib′-Expression Plasmid. The plasmid pA3A6 with the fused gene *aac(3)-Ib/aac-(6′)-Ib′* in the pGEM-T vector was a generous gift from Dr. Véronique Dubois (*10*). The expression plasmid was constructed similarly to what was described in a recent publication (*9*). In order to insert the gene into the expression vector pET22b(+) restriction enzyme sites of *Nde*I and *Eco*RI, it was first amplified by PCR with two primers, PETAAC-S (5′-GTTGT<u>CATA**ATG**</u>TTATGGAGCAGCAACGA-3′) and PETAAC-E (5′-CGATG<u>GAATTC</u>**TTA**GGCATCACTGCGT-

* Corresponding author. Tel: (574) 631-2933. Fax: (574) 631-6652. E-mail: mobashery@nd.edu.

GTTCGCTC-3′). The recognition sequences for *Nde*I (CATATG) and *Eco*RI (GAATTC) endonucleases are underlined, and start codon (ATG) and stop codon (TTA; antisense sequence of TAA) are in bold. The PCR product was cleaned with MinElute PCR Purification Kit (QIAGEN Inc., Valencia, CA), digested with *Nde*I and *Eco*RI, and ligated into the corresponding sites of the pET22b(+) vector. The ligated DNA was used to transform *Escherichia coli* BL21 (DE3). The recombinant plasmids were isolated from several transformants, and DNA sequencing was performed by the CMMG Macromolecular Core Facility (Wayne State University, Detroit, MI) on both strands to verify the nucleotide sequences of the *aac(3)-Ib/aac(6′)-Ib′* gene. The recombinant plasmid was named pET-A3A6.

Construction of Plasmids Harboring the Genes aac(3)-Ib or aac(6′)-Ib′. The plasmids pET-A3 and pET-A6, respectively harboring the *aac(3)-Ib* and *aac(6′)-Ib′* gene segments from the pET22b(+) vector, were constructed by PCR and ligation. For cloning of the *aac(3)-Ib* gene, the gene was amplified by PCR from pET-A3A6 with the following primers: PETA3-S 5′-GTTGTCATA**ATG**TTATGGAGCAG-CAACGA-3′ and PETA3-E 5′-TTGCT**GAATTCTTA**TG-GATCAATGTCGAAGTGCATGACG-3′ (recognition sites for *Nde*I and *Eco*RI endonucleases are underlined, and start codon (ATG) and stop codon (TTA) are in bold). The stop codon was incorporated at the 3′-end of the *aac(3)-Ib* gene. The *aac(6′)-Ib′* gene segment was also amplified by PCR from pET-A3A6 with the following primers: PETA6-S 5′-GACATT**CATATG**TTGACCAACAGCAACGATTCCG-TCAC-3′ and PETA6-E 5′-CGATG**GAATTCTTA**GGCAT-CACTGCGTGTTCGCTC-3′ (recognition sequences for *Nde*I and *Eco*RI endonucleases are underlined, and start (ATG) and stop (TTA) codons are in bold). One start codon was additionally incorporated for the initiation of translation of the *aac(6′)-Ib′* gene, as shown in the nucleotide sequence of the primer PETA6-S. The subsequent procedures for plasmid isolation and sequencing were the same as described above.

Expression and Purification of AAC(3)-Ib, AAC(6′)-Ib′, and AAC(3)-Ib/AAC(6′)-Ib′. In order to purify the AAC(6′)-Ib′ domain, a 5 mL overnight culture of *E. coli* BL21 (DE3) harboring the plasmid pET-A6 was inoculated into 500 mL of Luria–Bertani (LB) medium containing 100 μg/mL of ampicillin and incubated at 37 °C with shaking at 150 rpm. The expression of the protein was induced by the addition of isopropyl β-D-1-thiogalactopyranoside (IPTG) when the OD_{600} of the culture reached 0.6. The final IPTG concentration was 0.2 mM, and the growth was allowed for a duration of 20 h at 20 °C. Cells were harvested by centrifugation at 5500*g* for 30 min at 4 °C, washed with 50 mL of 10 mM Tris, pH 7.5, and resuspended in 30 mL of 10 mM Tris, pH 7.5. Cells were disrupted during 15 min of sonication using a Branson Sonifier 450 (VWR, West Chester, PA). After centrifugation at 21000*g* for 1 h at 4 °C, the supernatant was loaded onto a DEAE anion-exchange column with a rigid methacrylate polymer as a matrix (2.5 × 20 cm; Bio-Rad, Hercules, CA). The column was washed at a flow rate of 4 mL/min with 300 mL of 10 mM Tris, pH 7.5, and the proteins were eluted by a linear gradient of 0–1.0 M NaCl (900 mL). Fractions containing proteins were analyzed by sodium dodecyl sulfate–polyacrylamide gel electrophoresis (SDS–PAGE), and those containing proteins of approximately 22 kDa (deduced from the nucleotide sequence) were

pooled and concentrated using an Amicon ultrafiltration system and dialyzed against 2 L of buffer A (25 mM HEPES, pH 7.5 and 1 mM EDTA). The protein solution was loaded at a flow rate of 1.5 mL/min onto a kanamycin-affinity column [2.5 × 10 cm; 50 mL of Affi-Gel 15 resin (Bio-Rad, Hercules, CA)], prepared as described previously (*16*). The column was washed with 150 mL of buffer A, followed by a linear gradient of 0–1.0 M NaCl in buffer A (600 mL). The desired protein was finally eluted with buffer A containing 1.5 M NaCl. Homogeneity of the purified protein was confirmed by SDS–PAGE.

The AAC(3)-Ib domain was purified as follows. The cells were grown similarly, except the induction was performed by 2 g/L The Inducer (MoleculA, Columbia, MD; molarity cannot be calculated as the structure of the molecule is proprietary). Cells were harvested and disrupted as described above, followed by centrifugation at 21000*g* for 1 h at 4 °C. The supernatant was applied to a DEAE anion-exchange chromatography. The column was washed with 200 mL of 10 mM Tris, pH 7.5, at 4 mL/min of a flow rate, and then the proteins were eluted by a linear gradient of 0–1.0 M NaCl (800 mL). Fractions containing the AAC(3)-Ib domain of approximately 19 kDa (deduced from the nucleotide sequence) were analyzed by SDS–PAGE, were concentrated with an Amicon untrafiltration system, and were dialyzed with 2 L of buffer A. The dialyzed solution was loaded onto a gentamicin-affinity column at a flow rate of 1.5 mL/min. The column was first washed with 150 mL of buffer A, and the proteins were eluted by a linear gradient of 0–1.0 M NaCl in buffer A (600 mL). Fractions containing the AAC-(3)-Ib domain were checked by SDS–PAGE, were concentrated to a small volume, and were dialyzed against 10 mM sodium phosphate, pH 7.5. The protein was further purified with a Sephacryl-200 size-exclusion column at a flow rate of 0.3 mL/min.

For the purification of the full-length AAC(3)-Ib/AAC-(6′)-Ib′ enzyme, a 5 mL overnight culture of *E. coli* BL21 (DE3) cells harboring the pET-A3A6 plasmid was inoculated into 500 mL of Terrific Broth (TB) medium containing 100 μg/mL of ampicillin and incubated at 37 °C with shaking at 150 rpm. The expression of the protein was induced by the addition of 0.4 mM IPTG once the OD_{600} had reached 0.6. The cells were grown for an additional 24 h at 15 °C. Cells were harvested and disrupted as described above, followed by centrifugation at 21000*g* for 1 h at 4 °C. The supernatant was applied to a DEAE-anion exchange chromatography column. The column was washed with 300 mL of 10 mM Tris buffer, pH 7.5 at a 4 mL/min flow rate, and proteins were eluted with a linear gradient of 0–1.0 M NaCl (900 mL). Fractions containing the full length enzyme were identified by SDS–PAGE, pooled and concentrated to 5 mL, and dialyzed against 2 L of buffer A. The dialyzed solution was applied to a gentamicin-affinity column and purified as described above. Fractions containing the full-length protein were identified by SDS–PAGE, pooled and concentrated by an Amicon Ultra-15 Centrifugal Filter device (with molecular weight cutoff of 10 kDa), and dialyzed against 4 L of buffer A. The sample was frozen at this point for future use.

Enzymic Synthesis and Purification of Acetylated Kana-mycin A. The synthesis and purification of the acetylated kanamycin A were performed as described before (*9*). For

acetylation of kanamycin A (**1**) by AAC(6′)-Ib′ the reaction mixture contained 50 mM HEPES, pH 7.5, 3 mM acetyl-CoA, 2 mM kanamycin A, and 0.5 mg of AAC(6′)-Ib′ in a total volume of 50 mL. The mixture was incubated at room temperature for 6 h with gentle stirring. Additional portions of the enzyme (0.2 mg) were added into the mixture every 2 h. The reaction was monitored by thin-layer chromatography (TLC) using a mixture of ethanol−methanol−ammonia−water (5:5:4.5:4.5) as the developing solvent and ninhydrin as the visualization agent (*4*). After the reaction reached completion, the enzyme was removed from the reaction mixture by filtration through an Amicon ultrafiltration system (MWCO: 5000) and the filtrate was concentrated by rotary evaporation. The residue was suspended in 5 mL of water and loaded on silica gel packed in a 30 mL fritted glass filter (3 × 4 cm). Silica gel was washed with 150 mL of methanol−water (1:1) to remove acetyl-CoA and coenzyme A (CoASH). The product of the enzymic reaction was eluted from silica gel with 50 mL of the methanol−water−ammonia (1:1:0.5). The eluent was then concentrated and applied to a weak cation-exchange Amberlite CG-50 column (NH_4^+ form, 1.5 × 12 cm, Sigma-Aldrich). The column was washed with 100 mL of water, and a stepwise gradient of NH_4OH solution (0.25, 0.5, 0.75, 1.0, 1.5, 2.0, and 5.0%; 20 mL for each step) was utilized to elute acetylated kanamycin A. The desired product was eluted at 1.0% NH_4OH solution. It was concentrated to a small volume (2 mL) and was then lyophilized.

Enzymic Synthesis and Purification of Acetylated Fortimicin A. Acetylated fortimicin A was synthesized and purified essentially by the same method as described above. The reaction mixture contained 25 mM HEPES, pH 6.5, 2 mM acetyl-CoA, 1.5 mM fortimicin A, and 0.7 mg of AAC(3)-Ib in a total volume of 50 mL. The mixture was incubated at room temperature for 8 h with gentle agitation. Additional portions of the enzyme (0.2 mg) were added into the mixture every 3 h. During the weak cation-exchange chromatography step, acetylated fortimicin A was eluted at 0.5% NH_4OH solution.

NMR analyses of the Structurally Modified Aminoglycosides. The lyophilized samples were dissolved in D_2O. All ^{1}H and ^{13}C NMR experiments were performed as previously described (*9*) using Varian Unity*Plus* and Inova spectrometers operating at ^{1}H resonance frequency of 599.89 and 499.87 MHz, respectively. Various 1D and 2D homo- and heteronuclear NMR techniques including [13]C[^{1}H], APT (Attached Proton Test), [1]H−^{1}H COSY, [1]H−[1]H TOCSY, [1]H−[1]H ROESY, [1]H−[13]C HETCOR, [1]H−[13]C gHMQC, [1]H−[13]C gHMQCTOCSY, and [1]H−^{13}C gHMBC were utilized to elucidate the structures of the acetylated kanamycin A and the acetylated fortimicin A. Standard pulse sequences were used in these experiments (*17−22*). The Varian VNMR 6.1C software was used to process all spectra. [1]H spectra and the [1]H-dimension in 2D heteronuclear spectra were referenced relative to the signal of d_4-TMSP (internal standard, $\delta = 0$ ppm). [13]C spectra and the ^{13}C-dimension in the 2D heteronuclear spectra were referenced indirectly (*23*). The chemical structure of the acetylated kanamycin A was successfully assigned by NMR experiments.

The same procedures in analysis of the product of acetylation of fortimicin A revealed the existence of two inseparable acetylated fortimicin A derivatives. The mixture

was analyzed, and the structural nature of one of the two products was elucidated.

Kinetic Assays of the AAC(3)-Ib Domain, the AAC(6′)-Ib′ Domain, and the AAC(3)-Ib/AAC(6′)-Ib′. The catalytic activity of AAC(3)-Ib was measured spectrophotometrically by coupling the production of the sulfhydryl group of CoASH, generated by the AAC(3)-Ib activity, to the chemical reaction with 4,4′-dithiodipyridine (DTDP). The reaction progress was monitored continuously at 324 nm ($\Delta\epsilon = 19{,}800$ M^{-1} cm^{-1} for free pyridine-4-thiolate) (*14, 24, 25*). The assay mixture contained 50 mM HEPES, pH 6.5, 1 mM EDTA, 1 mM DTDP, 70 nM AAC(3)-Ib, and variable concentrations of aminoglycoside (2−20 μM) or acetyl-CoA (2−40 μM) in a total volume of 0.5 mL. For the assay of AAC(6′)-Ib′ the reaction mixture included 50 mM HEPES, pH 7.5, 1 mM EDTA, 1 mM DTDP, varied aminoglycoside (0.5−10 μM) or acetyl-CoA (10−80 μM), and 20 nM AAC(6′)-Ib′ in a total volume of 0.5 mL.

The initial velocity pattern for the AAC(3)-Ib domain was obtained at variable concentrations of gentamicin (from 2 to 20 μM) with three different concentrations of acetyl-CoA (2, 4, and 10 μM). The pattern was observed at varied kanamycin A (1−10 μM) and acetyl-CoA (10, 30, and 80 μM) for the AAC(6′)-Ib′ domain.

Inhibition Studies. The acetyltransferase activity of the AAC(3)-Ib domain was measured in the presence of the dead-end inhibitors, butyryl-CoA and dibekacin, or the product inhibitors, coenzyme A (CoASH) and acetylated fortimicin (AcFOR). The inhibition experiments were performed by varying the concentrations of one substrate at several different fixed concentrations of the inhibitor, while the other substrate was kept at a constant concentration. The reaction progress was monitored at 324 nm as in the standard kinetic assay, except for the product inhibition experiment by CoASH. The pattern of the product inhibition by CoASH was obtained by monitoring the decrease in absorbance at 232 nm ($\Delta\epsilon = 4500$ M^{-1} cm^{-1}), due to the breakage of the thioester bond of acetyl-CoA (*14*). Inhibition of the acetyltransferase activity for the AAC(6′)Ib′ domain was also determined similarly in the presence of dead-end inhibitors (butyryl-CoA and paromomycin) and product inhibitors (CoASH and acetylated kanamycin).

Solvent-Isotope Effects. The solvent-isotope effects on k_{cat} and k_{cat}/K_m of AAC(3)-Ib were determined not only at varied concentrations of gentamicin (2−20 μM) and the saturating concentration (100 μM) of acetyl-CoA but also at various concentrations of acetyl-CoA (2−20 μM) with the fixed concentration of gentamicin (100 μM). The experiments were performed at two different pD values of 6.5 and 7.5. The solvent-isotope effects of AAC(6′)-Ib′ were determined at varied concentrations of kanamycin A (1−8 μM) with a fixed concentration of acetyl-CoA (100 μM) and at various concentrations of acetyl-CoA (10−100 μM) with a fixed concentration of kanamycin (5 μM). The experiment was only performed at pD 7.5 due to the limited pH window of activity for the AAC(6′)-Ib′ domain (data not given). The reaction mixtures contained approximately 97% deuterium oxide. The value of pD was adjusted by adding 0.4 unit to the pH value measured with a pH meter (*26, 27*).

Data Analysis. Data of steady-state kinetics were fitted to eq 1 using Grafit 4.0 software (Erithacus Software, U.K.). Equation 2 was used to fit the initial velocity patterns. All

data of the inhibition studies were fitted to eqs 3, 4, and 5 for competitive, uncompetitive, and noncompetitive/mixed inhibition, respectively (*28*, *29*).

$$v = V_m[A]/(K_a + [A]) \qquad \text{(eq 1)}$$

$$v = V_m[A][B]/(K_a[B] + K_b[A] + [A][B] + K_{ia}K_b) \quad \text{(eq 2)}$$

$$v = V_m[A]/([A] + K_a(1 + [I]/K_{is})) \qquad \text{(eq 3)}$$

$$v = V_m[A]/(K_a + [A](1 + [I]/K_{ii})) \qquad \text{(eq 4)}$$

$$v = V_m[A]/(K_a(1 + [I]/K_{is}) + [A](1 + [I]/K_{ii})) \qquad \text{(eq 5)}$$

In all equations, v is the initial velocity, V_m is the maximum velocity, [A] and [B] are the concentrations of substrates, [I] is the concentration of inhibitor, K_a and K_b are the corresponding Michaelis–Menten constants, K_{ia} is the dissociation constant for A, and K_{is} and K_{ii} are the slope and intercept inhibition constants for inhibitors, respectively, and are evaluated by replotting the slope and the intercept from double-reciprocal plots, respectively, versus the concentration of inhibitor.

RESULTS AND DISCUSSION

The *aac(3)-Ib/aac(6′)-Ib′* gene encoding the bifunctional enzyme was amplified by PCR from plasmid pA3A6, and its nucleotide sequence was determined (three individual experiments). We found one difference, from nucleotide G589 to C (corresponding to a Val → Leu amino acid substitution; in the *aac(6′)-Ib′* gene segment) in the sequence from our experiments compared to that reported earlier (GenBank accession number AF355189) (*10*). Subsequently, nucleotide sequencing with the *aac(3)-Ib/aac(6′)-Ib′* gene in the plasmid pA3A6 was performed in order to see if the discrepancy was also present in the original gene, which turned out to be the case. Since independent sequencing of each PCR product and the original plasmid were performed three times each in our lab, the original sequence report appeared to contain an inadvertent error. The PCR products for the independently cloned *aac(3)-Ib* and *aac(6′)-Ib′* gene segments from pET-A3A6 possessed the identical nucleotide sequences to the parental sequence of the bifunctional gene.

We prepared the plasmid pET-A3A6 for overexpression of AAC(3)-Ib/AAC(6′)-Ib′. The expression of AAC(3)-Ib/AAC(6′)-Ib′ in *E. coli* BL21 (DE3) was tested with different concentrations of IPTG (0.05, 0.1, 0.2, and 0.4 mM) and The Inducer (a commercial alternative to IPTG; 0.5, 1, 2, and 4 g/L) at 20 °C to determine appropriate concentration of the inducing agents that result in the soluble protein. All attempts at expression of the full-length AAC(3)-Ib/AAC-(6′)-Ib′ with IPTG resulted in precipitated protein with high levels of expression, while The Inducer produced modest amounts of the soluble AAC(3)-Ib/AAC(6′)-Ib′, with the best result at 2 g/L (data not shown).

Since both domains of AAC(3)-Ib/AAC(6′)-Ib′ possess acetyltransferase activities, it was necessary to separate the protein in its two domains to investigate the mechanism of each independently. We constructed expression vectors for each domain. The expression level of each domain was determined with 0.2 mM IPTG and 2 g/L of The Inducer at 20 °C. Both IPTG and The Inducer produced large quantities of soluble AAC(6′)-Ib′, while AAC(3)-Ib precipitated as
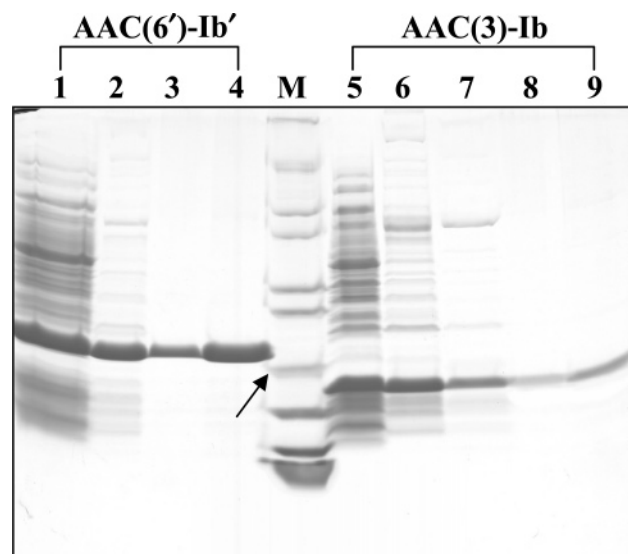

FIGURE 1: SDS–PAGE for the purification of the AAC(6′)-Ib′ and AAC(3)-Ib domains. Lane 1, crude extract containing AAC(6′)-Ib′; lane 2, the protein pool after the DEAE anion-exchange chromatography; lanes 3 and 4, pure AAC(6′)-Ib′ after the kanamycin-affinity chromatography; lane 5, crude extract containing AAC(3)-Ib; lane 6, the protein pool after the DEAE anion-exchange chromatography; lane 7, the protein pool after the gentamicin-affinity chromatography; and lanes 8 and 9, AAC(3)-Ib after the size-exclusion chromatography. M indicates the molecular size marker, with the following molecular weights for each band from the top to the bottom: 200, 116.3, 97.4, 66.3, 55.4, 36.5, 31.0, 21.5, 14.4, 6.0, and 3.5 kDa. The arrow indicates 21.5 kDa.

inclusion bodies even though its expression level was somewhat lower than that of AAC(6′)-Ib′ with either inducer (data not shown). Homogeneous AAC(6′)-Ib′ and AAC(3)-Ib were obtained by a two-step and a three-step purification procedure, respectively (60 and 12 mg per liter of cell culture, respectively; Figure 1).

The analyses of the nucleotide and the deduced protein sequences by Dubois et al. had suggested that the enzyme should have two aminoglycoside acetyltransferase (AAC) activities (*10*). The types of the enzymic reactions could be deduced from the protein sequence comparisons with those of the other known members of a class; however, such analyses should be followed up by actual determination of the chemical structures of the products. We undertook this effort.

The minimum inhibitory concentration (MIC) investigations of Dubois et al. (*10*) indicated that the bacteria harboring the gene for the bifunctional enzyme exhibited resistance to several aminoglycoside antibiotics, of which we chose fortimicin A and kanamycin A for characterization of the reactions of the two domains (Figure 2). The two enzymic reactions were allowed to progress to completion, and then the products were purified by chromatographic procedures, followed by structural assignments of the products, as described in the Experimental Procedures. The structures of the products were determined by analysis of 1D and 2D ^{1}H and ^{13}C NMR spectroscopy. Proton connectivities were derived by examination of the COSY and TOCSY spectra. Signals of all carbons with direct proton attachments were assigned using HETCOR and gHMQC spectra. Finally, the gHMBC and gHMQC-TOCSY spectra were used to assign quaternary carbons and to check the correctness of the connectivities established by the interpreta-
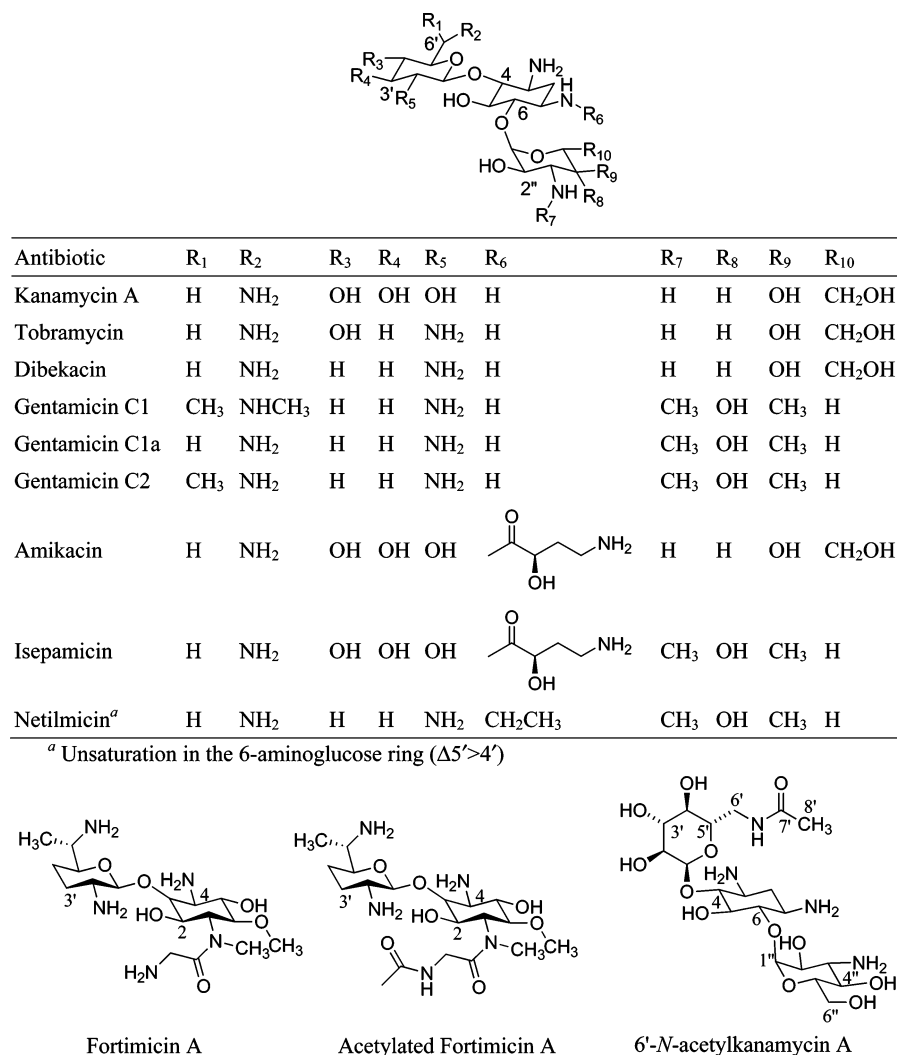
Antibiotic	R_1	R_2	R_3	R_4	R_5	R_6		R_7	R_8	R_9	R_{10}
Kanamycin A	H	NH_2	OH	OH	OH	H		H	H	OH	CH_2OH
Tobramycin	H	NH_2	OH	H	NH_2	H		H	H	OH	CH_2OH
Dibekacin	H	NH_2	H	H	NH_2	H		H	H	OH	CH_2OH
Gentamicin C1	CH_3	$NHCH_3$	H	H	NH_2	H		CH_3	OH	CH_3	H
Gentamicin C1a	H	NH_2	H	H	NH_2	H		CH_3	OH	CH_3	H
Gentamicin C2	CH_3	NH_2	H	H	NH_2	H		CH_3	OH	CH_3	H
Amikacin	H	NH_2	OH	OH	OH	(4-amino-2-hydroxybutanoyl)		H	H	OH	CH_2OH
Isepamicin	H	NH_2	OH	OH	OH	(4-amino-2-hydroxybutanoyl)		CH_3	OH	CH_3	H
Netilmicin[a]	H	NH_2	H	H	NH_2	CH_2CH_3		CH_3	OH	CH_3	H

[a] Unsaturation in the 6-aminoglucose ring ($\Delta 5'>4'$)

Fortimicin A   Acetylated Fortimicin A   6'-*N*-acetylkanamycin A

FIGURE 2: Structures of aminoglycoside antibiotics and that of 6'-*N*-acetylkanamycin A.

tion of the other spectra. ^{1}H and ^{13}C spectra of the modified kanamycin A were identical to those of 6'-*N*-acetyl-kanamycin A, as described previously in connection with the studies of another enzyme (Figure 2) (*9*). This AAC activity transfers the acetyl group from acetyl-CoA to the 6'-amine of kanamycin A; therefore, it was correctly designated as an AAC(6').

Analyses of the turnover product(s) of fortimicin A proved problematic. The product mixture was made up of two compounds that could not be separated; hence we could not carry out unequivocal structure assignments because of the complexities of the spectra for the mixture (product isolation was performed twice). Nonetheless, the full assignment of the ^{1}H and ^{13}C NMR spectra for fortimicin was made, and it was helpful in identifying one of the sites of acetylation as the glycyl amine (α to the amide carbonyl). This assignment was made based on the observation of the complete loss of the resonance at δ 163.9 for the amide carbonyl of fortimicin A, which indicated that the electron withdrawing inductive effect of the acetylation at the aminomethyl moiety shifted the carbonyl resonance to a new position. The product mixture showed a minimum of four carbonyl resonances in the range δ 174.3 and 173.2, two due to the amide carbonyls and the additional two due to the acetyl groups that were incorporated into the products.

Regardless of the absence of regiospecificity, the reaction progress with fortimicin A was monophasic, suggesting that the two amines were acetylated with similar rate constants by the domain designated as AAC(3)-Ib. The possibility of modification of the substrate at more than one site is not unprecedented for aminoglycoside-modifying enzymes. This domain also takes gentamicin as its substrate. However, the structural assignment for the acetylated gentamicin was not attempted, as the commercial gentamicin is a mixture of three closely related aminoglycosides, gentamicins C1, C1a, and C2. Furthermore, netilmicin, the other substrate for this domain, is a very poor substrate, and it was not practical to isolate the product for its reaction.

This domain had been assigned as AAC(3)-Ib by the Dubois group from analysis of the sequence of the domain (*10*). Since we were not able to identify the second site of acetylation in fortimicin A, we do not have any basis to challenge the enzyme designation and we will continue to refer to the domain as AAC(3)-Ib.

Since both domains carry out acetyltransferase reactions, it was necessary for mechanistic studies to characterize each separately. Hence, the two domains were cloned separately and purified to homogeneity. Table 1 presents the steady-state kinetic parameters for the reactions catalyzed by the AAC(3)-Ib and AAC(6')-Ib' domains. The AAC(3)-Ib do-

Table 1: Steady-State Kinetic Parameters for the AAC(3)-Ib and AAC (6′)-Ib′ Domains[a]

substrate	AAC(3)-Ib			AAC(6′)-Ib′		
	k_{cat} (s^{-1})	K_m (μM)	k_{cat}/K_m (M^{-1} s^{-1})	k_{cat} (s^{-1})	K_m (μM)	k_{cat}/K_m (M^{-1} s^{-1})
fortimicin A	0.18 ± 0.01	3.3 ± 0.9	(5.4 ± 1.5) × 10^4	ns[b]	ns	ns
gentamicin[c]	0.28 ± 0.01	3.5 ± 0.2	(7.9 ± 0.6) × 10^4	2.0 ± 0.2	8.3 ± 2.1	(2.0 ± 0.1) × 10^5
netilmicin	0.05 ± 0.01	140 ± 30	(3.4 ± 0.7) × 10^2	1.3 ± 0.1	1.0 ± 0.2	(2.0 ± 0.5) × 10^6
amikacin	ns	ns	ns	3.5 ± 0.2	1.0 ± 0.2	(4.0 ± 0.7) × 10^6
dibekacin	ns	ns	ns	1.3 ± 0.1	3.0 ± 0.5	(5.0 ± 1.0) × 10^5
isepamicin	ns	ns	ns	2.4 ± 0.1	0.3 ± 0.1	(8.0 ± 1.1) × 10^6
kanamycin A	ns	ns	ns	2.4 ± 0.1	1.0 ± 0.1	(2.4 ± 0.3) × 10^6
neomycin	ns	ns	ns	6.0 ± 0.4	1.2 ± 0.3	(5.0 ± 1.2) × 10^6
acetyl-CoA[d]	0.28 ± 0.02	3.0 ± 0.6	(9.4 ± 2.1) × 10^4	1.0 ± 0.1	9.0 ± 4.0	(1.0 ± 0.5) × 10^5

[a] The following kinetic parameters were measured for the purified full-length bifunctional enzyme: fortimicin A, $k_{cat} = 0.13 \pm 0.03$ s^{-1}, $K_m = 3.7 \pm 0.2$ μM, and $k_{cat}/K_m = (3.5 \pm 0.2) \times 10^4$ M^{-1} s^{-1}; and kanamycin A, $k_{cat} = 3.0 \pm 0.3$ s^{-1}, $K_m = 9.1 \pm 1.5$ μM, and $k_{cat}/K_m = (3.3 \pm 0.6) \times 10^5$ M^{-1} s^{-1}. [b] Not substrate. [c] The commercially available gentamicin is a mixture of gentamicin C1 (~35%), C1a (~35%), and C2 (~ 30%). [d] Kinetic parameters for acetyl-CoA were determined at the fixed concentration of gentamicin (100 μM) for AAC(3)-Ib and kanamycin A (10 μM) for AAC(6′)-Ib′, as described in the Experimental Procedures.

main carried out acetylation of gentamicin and fortimicin A with k_{cat}/K_m values of (7.9 ± 0.6) × 10^4 M^{-1} s^{-1} and (5.4 ± 1.5) × 10^4 M^{-1} s^{-1}, respectively. As stated earlier, the kinetics were monophasic and linear for both gentamicin and fortimicin A, even though gentamicin is a mixture of three closely related components and fortimicin A was acetylated at two amines. Netilmicin was a poor substrate for AAC-(3)-Ib with k_{cat}/K_m value of (3.4 ± 0.7) × 10^2 M^{-1} s^{-1}, with both attenuated k_{cat} and elevated K_m, compared to the other two substrates. This domain exhibited high specificity for gentamicin and fortimicin A, that is, it did not acetylate spectinomycin (a representative atypical aminoglycoside), all other 4,6-disubstituted 2-deoxystreptamine aminoglycosides tested (amikacin, dibekacin, isepamicin, kanamycin A, and tobramycin), and 4,5-disubstituted antibiotics such as neomycin and paromomycin. This finding is consistent with microbiological aminoglycoside resistance patterns reported earlier (10). We also discovered that none of the aminoglycosides inhibited the AAC(3)-Ib activity except for dibekacin. The structural difference between dibekacin and kanamycin A or tobramycin is only the presence of a hydroxyl group at C-3′ (R4) or C-4′ (R3), as depicted in Figure 2. In spite of this small difference, only dibekacin inhibits the reaction catalyzed by AAC(3)-Ib, but kanamycin A and tobramycin do not. Acetyl-CoA is the second substrate, the donor of the acetyl group. It exhibited a K_m of 3.0 ± 0.6 μM for AAC-(3)-Ib, a rather low value compared to other AAC enzymes (15, 24, 30, 31). Butyryl-CoA, used for the inhibition studies, was not a substrate for this domain. There was no evidence of substrate inhibition with either aminoglycosides or acetyl-CoA.

In contrast to the AAC(3)-Ib domain, AAC(6′)-Ib′ domain exhibited a broad substrate preference, including many 4,6-disubstituted aminoglycosides (amikacin, dibekacin, gentamicin, isepamicin, and kanamycin A) and one 4,5-disubstituted aminoglycoside, neomycin (Table 1). Another 4,5-disubstituted aminoglycoside, paromomycin, was not a substrate, hence we used it as a dead-end inhibitor. The AAC-(6′)-Ib′ domain utilized only acetyl-CoA as the acetyl donor, with K_m of 9.0 ± 4.0 μM. Butyryl-CoA was used as a dead-end inhibitors for AAC(6′)-Ib′, since it was not a substrate. It has been proposed that the AAC(6′)-I family would not acetylate gentamicin, but would amikacin (32−34). Surprisingly the AAC(6′)-Ib′ domain acetylates both gentamicin [$k_{cat}/K_m = (2.0 \pm 0.1) \times 10^5$ M^{-1} s^{-1}] and amikacin [$k_{cat}/K_m = (4.0 \pm 0.7) \times 10^6$ M^{-1} s^{-1}] more readily than other AAC-(6′) enzymes, including the AAC(6′)-II family members (5, 9, 24), even though the nucleotide sequence for this domain exhibited 99% identity to that for $aac(6′)$-Ib′ gene. Acetylation of gentamicin by an AAC(6′)-I was reported by Wright and Ladak with AAC(6′)-Ii (24) and Daigle et al. with the bifunctional AAC(6′)-Ie/APH(2) (5). Therefore a closer structural investigation of the active site of the AAC(6′)-Ib′ domain is required to elucidate divergence of the substrate spectrum among AAC(6′)-I enzymes.

With the reactions for each domain defined, we also purified the bifunctional enzyme for comparison to the results of the individual domains for turnover of two substrates, fortimicin A and kanamycin A (Table 1). The AAC(3)-Ib domain in the bifunctional enzyme exhibited a similar k_{cat}/K_m value of (3.5 ± 0.2) × 10^4 M^{-1} s^{-1} compared to (5.4 ± 1.5) × 10^4 M^{-1} s^{-1} of the free-standing AAC(3)-Ib domain. However, the AAC(6′)-Ib′ domain exhibited an approximately 10-fold diminished k_{cat}/K_m value from (2.4 ± 0.3) × 10^6 M^{-1} s^{-1} to (3.4 ± 0.6) × 10^5 M^{-1} s^{-1} due to increase in the K_m value for the full-length enzyme. Hence, fusion of the two domains actually attenuates the activity of one domain somewhat, but does not affect the other.

We subsequently investigated the kinetic mechanisms of the AAC(3)-Ib and AAC(6′)-Ib′ domains. For preliminary determination of the kinetic mechanism, initial velocity patterns of catalysis by each domain were examined using various concentrations of gentamicin (2, 4, 10, and 40 μM) at different fixed concentrations of acetyl-CoA (2, 4, 10, and 20 μM) for the AAC(3)-Ib domain and using kanamycin A (3, 5, 7, and 10 μM) and acetyl-CoA (10, 30, and 80 μM) for the AAC(6′)-Ib′ domain. The double-reciprocal plots exhibited intersecting lines for the enzymic reactions, indicative of a sequential kinetic mechanism, either random or ordered (Figure 3). Both substrates, acetyl-CoA and aminoglycoside, would be bound to the enzyme before the formation and release of the two products. The sequential kinetic mechanism (random or ordered) appears to hold true for all classes of aminoglycoside-modifying enzymes (9, 14, 25, 28, 30, 35−43).

The detailed kinetic mechanisms of an enzymic reaction can be elucidated by the determination of the order of substrate binding or product release, as well as the determination of the rate-limiting step in catalysis. Investigations with dead-end and product inhibitors are useful methods to
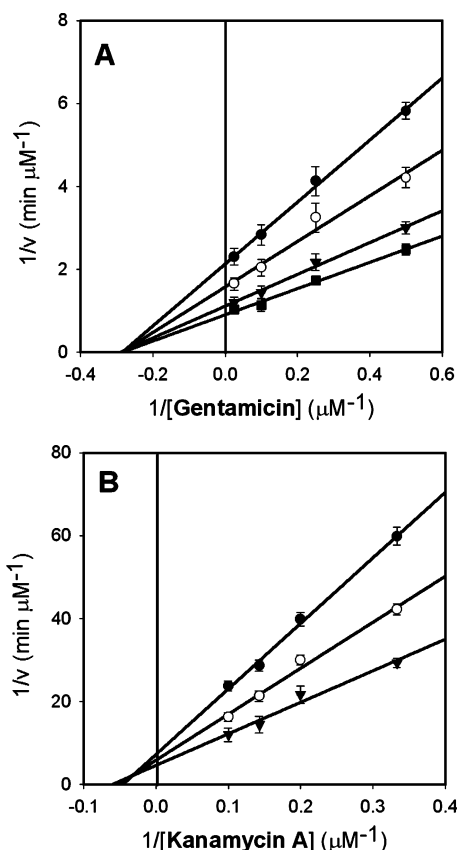
FIGURE 3: The initial velocity patterns for the AAC(3)-Ib and AAC-(6′)-Ib′-catalyzed reactions. (A) the initial velocity pattern for AAC-(3)-Ib was obtained at varied concentrations of gentamicin (from 2 to 40 μM) with several fixed concentrations of acetyl-CoA of 2 μM (●), 4 μM (○), 10 μM (▼), and 20 μM (■). (B) The initial velocity pattern for AAC(6′)-Ib′ measured at varied kanamycin A (from 1 to 10 μM) with three constant concentrations of acetyl-CoA at 10 μM (●), 30 μM (○), and 80 μM (▼). The patterns for the analyses with both domains are intersecting, indicative of sequential kinetic mechanisms for both domains. Each data point was determined in triplicate, and the error bars indicate the data spread in each case.

Table 2: Patterns of Dead-End and Product Inhibitions for the AAC(3)-Ib Domain

variable substrate[a]	inhibitor[b]	pattern of inhibition	K_{is} (μM)[c]	K_{ii} (μM)[c]
gentamicin	dibekacin	competitive	120 ± 10	
gentamicin	butyryl-CoA	no inhibition		
gentamicin	butyryl-CoA[d]	noncompetitive/ mixed	30 ± 2	40 ± 2
acetyl-CoA	dibekacin	no inhibition		
acetyl-CoA	dibekacin[d]	uncompetitive		270 ± 80
acetyl-CoA	butyryl-CoA	competitive	20 ± 4	
gentamicin	AcFOR	noncompetitive/ mixed	30 ± 2	30 ± 2
gentamicin	CoASH	noncompetitive/ mixed	110 ± 40	380 ± 120
acetyl-CoA	AcFOR	uncompetitive		50 ± 9
acetyl-CoA	CoASH	competitive	20 ± 4	

[a] These substrates were also used as the fixed substrates at 100 μM. [b] AcFOR, acetylated fortimicin A, and CoASH, coenzyme A. [c] K_{is} and K_{ii} were evaluated by replotting the slope and the intercept, respectively, from double reciprocal plots versus concentration of inhibitor. [d] Gentamicin or acetyl-CoA was used as the fixed substrate at 4 μM.

as the inhibitor versus gentamicin as the variable-concentration substrate with fixed unsaturating concentration for acetyl-CoA (4 μM) (Figure 4C). Uncompetitive inhibition of dibekacin and noncompetitive/mixed inhibition of butyryl-CoA with respect to acetyl-CoA and gentamicin, respectively, suggest that acetyl-CoA is the first substrate binding to the AAC(3)-Ib domain, followed by gentamicin (*29*). This conclusion is supported by the inhibition pattern of acetylated fortimicin A (AcFOR) versus acetyl-CoA, in which uncompetitive inhibition was observed, as described below.

Product-inhibition patterns complement these studies (*44*). Product-inhibition studies were performed with AcFOR and coenzyme A (CoASH). AcFOR exhibited noncompetitive/mixed inhibition (K_{is} = 30 ± 2 μM and K_{ii} = 30 ± 2 μM) versus gentamicin and uncompetitive inhibition (K_{ii} = 50 ± 9 μM) with respect to acetyl-CoA (Figure 5A and Figure 5B, respectively). CoASH inhibited the enzymic activity noncompetitively (K_{is} = 110 ± 40 μM and K_{ii} = 380 ± 120 μM; Figure 5C) and competitively (K_{is} = 20 ± 4 μM; Figure 5D) with respect to gentamicin and acetyl-CoA, respectively. These results indicate that AcFOR would be released from the active site prior to CoASH (*44*). The orders of substrate binding and product release for the AAC(3)-Ib domain are consistent with those of AAC(6′)-Ii from *Enterococcus faecium* (*41*), which follows an ordered Bi−Bi kinetic mechanism. Furthermore, uncompetitive inhibition by Ac-FOR (the first product to be released) with respect to acetyl-CoA (the first substrate) at the saturating concentration of gentamicin indicates that the catalytic reaction of the AAC-(3)-Ib domain follows a steady-state ordered Bi−Bi kinetic mechanism (*44*). This proposed mechanism is further supported by the result of the solvent-isotope effect analyses, as will be discussed later.

The dead-end and product inhibition studies for AAC(6′)-Ib′ domain were performed using paromomycin and butyryl-CoA as dead-end inhibitors and 6′-*N*-acetylkanamycin A (AcKAN) and CoASH as product inhibitors. The results of this study are presented in Table 3. Paromomycin, an aminoglycoside containing a 6′-hydroxyl group instead of an amino group, exhibited competitive inhibition (K_{is} = 1.2 ± 0.2 μM) versus kanamycin A (Figure 6A) and uncom-

elucidate whether the kinetic mechanism is ordered or random for the enzymic modifications of aminoglycosides by each of the AAC(3)-Ib and AAC(6′)-Ib′ domains, as well as the binding order of substrates and the releasing order of the products. In order to distinguish between the random and the ordered additions of the two substrates (gentamicin and acetyl-CoA) for AAC(3)-Ib, dead-end inhibition studies were carried out. The results of the inhibition studies are summarized in Table 2. As stated earlier, dibekacin was chosen as one of the dead-end inhibitors, since this compound alone among aminoglycosides inhibited AAC(3)-Ib. Dibekacin exhibited competitive (K_{is} = 120 ± 10 μM) and uncompetitive inhibitions (K_{ii} = 270 ± 80 μM) with respect to gentamicin (Figure 4A) and acetyl-CoA (Figure 4B), respectively. No inhibition by dibekacin with respect to acetyl-CoA was observed when gentamicin was used as a fixed substrate at the saturating concentration of 100 μM, while uncompetitive inhibition by this compound versus acetyl-CoA was demonstrated under fixed unsaturating concentration of gentamicin (4 μM). This inhibition pattern is seen when acetyl-CoA binds to the enzyme prior to gentamicin. A noncompetitive/mixed inhibition pattern (K_{is} = 30 ± 2 μM and K_{ii} = 40 ± 2 μM) was observed with butyryl-CoA
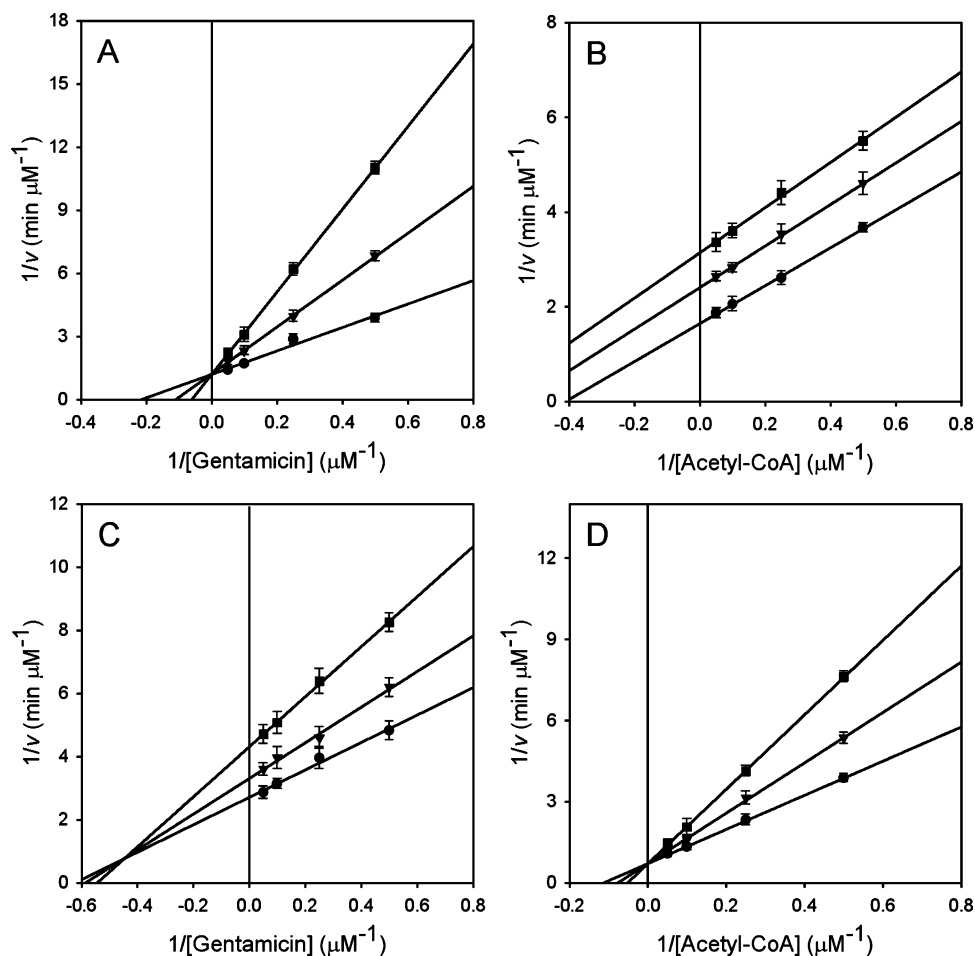
FIGURE 4: The inhibition patterns of dead-end inhibitors for the AAC(3)-Ib domain. (A) Competitive inhibition by dibekacin (●, 100 μM; ▼, 400 μM; ■, 800 μM) with respect to gentamicin (2−20 μM). (B) Uncompetitive inhibition by dibekacin (●, 100 μM; ▼, 200 μM; ■, 400 μM) with respect to acetyl-CoA (2−20 μM). (C) Noncompetitive/mixed inhibition by butyryl-CoA (●, 10 μM; ▼, 20 μM; ■, 40 μM) with respect to gentamicin (2−20 μM). (D) Competitive inhibition by butyryl-CoA (●, 10 μM; ▼, 20 μM; ■, 40 μM) with respect to acetyl-CoA (2−20 μM). Each data point was determined in triplicate, and the error bars indicate the data spread for each.

petitive inhibition ($K_{ii} = 40 \pm 6\,\mu$M) with respect to acetyl-CoA, respectively (Figure 6B). Butyryl-CoA showed noncompetitive/mixed ($K_{is} = 150 \pm 50\,\mu$M and $K_{ii} = 570 \pm 50\,\mu$M) and competitive ($K_{is} = 110 \pm 20\,\mu$M) inhibitions with respect to kanamycin A and acetyl-CoA, respectively (Figure 6C and Figure 6D). As documented earlier, uncompetitive inhibition of paromomycin versus acetyl-CoA indicates that acetyl-CoA is the first substrate binding to the AAC(6′)-Ib′ domain. The order of substrate binding for this domain is the same as that for the AAC(3)-Ib domain. In addition to dead-end inhibition, noncompetitive/mixed inhibitions were observed by one of two enzymic products, AcKAN, with respect to both kanamycin A ($K_{is} = 50 \pm 10\,\mu$M and $K_{ii} = 550 \pm 170\,\mu$M; Figure 7A) and acetyl-CoA ($K_{is} = 40 \pm 5\,\mu$M and $K_{ii} = 380 \pm 90\,\mu$M; Figure 7B). The other product CoASH exhibited noncompetitive/mixed ($K_{is} = 20 \pm 6\,\mu$M and $K_{ii} = 200 \pm 7\,\mu$M) and competitive ($K_{is} = 30 \pm 10\,\mu$M) inhibitions with respect to kanamycin A (Figure 7C) and acetyl-CoA (Figure 7D), respectively. The competitive inhibition pattern of CoASH versus acetyl-CoA may occur when CoASH competes with the first substrate acetyl-CoA in order to bind to the free form of AAC(6′)-Ib′. This pattern therefore indicates that CoASH is the last product to be released from the active site of AAC(6′)-Ib′. Moreover the noncompetitive/mixed inhibition pattern of AcKAN with

respect to kanamycin A eliminates the possibility of a Theorell−Chance Bi−Bi kinetic mechanism for the AAC-(6′)-Ib′-catalyzed reaction, because the first product (Ac-KAN) should exhibit competitive inhibition versus the second substrate kanamycin A in that kinetic mechanism (*44*). The results of inhibition studies suggest that, similar to the case of AAC(3)-Ib, AAC(6′)-Ib′ follows the steady-state ordered Bi−Bi kinetic mechanism, where acetyl-CoA binds first to the AAC(6′)-Ib′ domain followed by kanamycin A, and then the first product AcKAN is released from the enzyme prior to CoASH.

Analysis of solvent-isotope effects can be a powerful tool to identify which steps in the enzymic reaction would limit the overall rate of the reaction. The contribution of proton-transfer events to catalysis could be elucidated by solvent kinetic isotope effect. The measurement of solvent-isotope effects at two pD is necessary because pK_a values of potential catalytic residues may be perturbed by deuterium oxide (*39*). The solvent-isotope effect on catalysis by the AAC(3)-Ib domain was determined at pD values of 6.5 and 7.5 for gentamicin. The assays were carried out at fixed, saturating concentrations of acetyl-CoA with variable concentrations of gentamicin. The effects on k_{cat} for gentamicin at both pD values were identical and rather significant with a k_{cat}^{H}/k_{cat}^{D} value of 2.2 $\pm$ 0.2 (Table 4). The solvent-isotope effect on
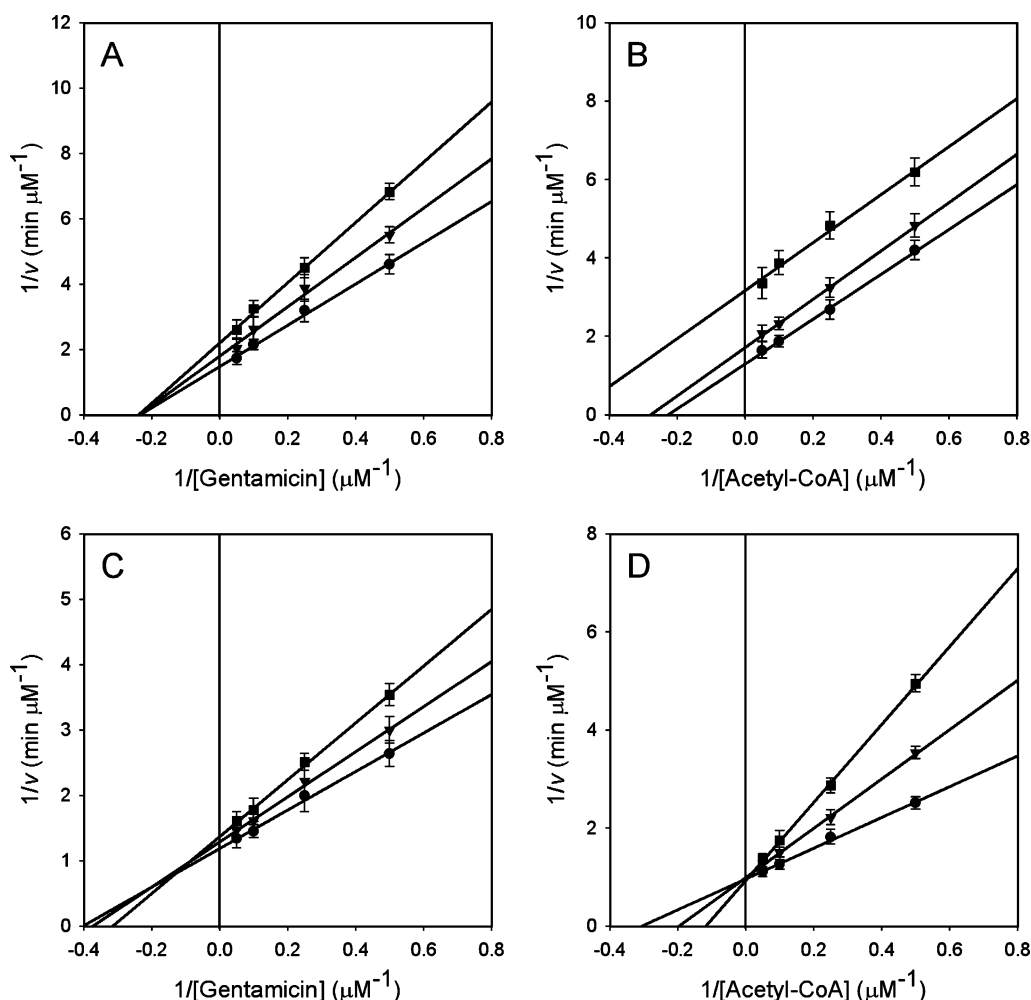
FIGURE 5: The inhibition patterns of the products for the AAC(3)-Ib domain. (A) Noncompetitive inhibition by acetylated fortimicin A (AcFOR; ●, 4 μM; ▼, 10 μM; ■, 20 μM) with respect to gentamicin (2−20 μM). (B) Uncompetitive inhibition by AcFOR (●, 10 μM; ▼, 40 μM; ■, 100 μM) with respect to acetyl-CoA (2−20 μM). (C) Noncompetitive/mixed inhibition by CoASH (●, 20 μM; ▼, 40 μM; ■, 80 μM) with respect to gentamicin (2−20 μM). (D) Competitive inhibition by CoASH (●, 20 μM; ▼, 40 μM; ■, 80 μM) with respect to acetyl-CoA (2−20 μM). Each data point was determined in triplicate, and the error bars indicate the data spread for each.

Table 3: Patterns of Dead-End and Product Inhibitions for the AAC (6′)-Ib′ Domain

variable substrate[a]	inhibitor[b]	pattern of inhibition	K_{is} (μM)[c]	K_{ii} (μM)[c]
kanamycin A	paromomycin	competitive	1.2 ± 0.1	
kanamycin A	butyryl-CoA	noncompetitive/ mixed	150 ± 50	570 ± 50
acetyl-CoA	paromomycin	uncompetitive		40 ± 6
acetyl-CoA	butyryl-CoA	competitive	110 ± 20	
kanamycin A	AcKAN	noncompetitive/ mixed	50 ± 10	550 ± 170
kanamycin A	CoASH	noncompetitive/ mixed	20 ± 6	200 ± 7
acetyl-CoA	AcKAN	noncompetitive/ mixed	40 ± 5	380 ± 90
acetyl-CoA	CoASH	competitive	30 ± 10	

[a] These substrates were also used as the fixed substrates (100 μM of acetyl-CoA and 10 μM of kanamycin A). [b] AcKAN, 6′-*N*-acetylated kanamycin A, and CoASH, coenzyme A. [c] K_{is} and K_{ii} were evaluated by replotting the slope and the intercept, respectively, from double reciprocal plots versus concentration of inhibitor.

k_{cat} for acetyl-CoA was measured at a pD of 6.5, resulting in a k_{cat}^{H}/k_{cat}^{D} value of 2.6 ± 0.3 The solvent-isotope effects of AAC(6′)-Ib′ domain for kanamycin A and acetyl-CoA were determined at pD 7.5 since this domain has a narrow pH range for the maximal activity and the variations in the

activity by pH change are smallest in this region (data not shown). The effects on k_{cat} of AAC(6′)-Ib′ for kanamycin A and acetyl-CoA were also considerable with k_{cat}^{H}/k_{cat}^{D} values of 2.7 ± 0.3 and 2.0 ± 0.4, respectively (Table 4). These results indicate that proton transfer may at least partially contribute to the overall rate in the reactions of both AAC-(3)-Ib and AAC(6′)-Ib′. As all of our results consistently suggest, both AAC(3)-Ib and AAC(6′)-Ib′ domains appear to follow an ordered Bi−Bi kinetic mechanism, where acetyl-CoA is the first substrate to bind the domains and coenzyme A is the final product to be released.

Over 50 unique aminoglycoside acetyltransferases have been identified so far (*34, 43*). Only a few AACs, including AAC(3)-I (*14*), AAC(3)-IV (*15*), AAC(2′)-Ic (*25*), AAC-(6′)/APH(2′′) (*35*), AAC(6′)-Iy (*30*), AAC(6′)-Ii (*41*), and ANT(3′′)-Ii/AAC(6′)-IId (*9*), have been investigated for their kinetic mechanisms. All AAC enzymes studied follow the random sequential kinetic mechanism, except AAC(6′)-Ii and ANT(3′′)-Ii/AAC(6′)-IId, which follow the ordered Bi−Bi kinetic mechanism. These two AACs have different orders of substrate binding and product releasing. AAC(6′)-Ii follows an ordered Bi−Bi ternary complex mechanism, where acetyl-CoA binds first to the enzyme followed by the aminoglycoside. This is followed by the release of the
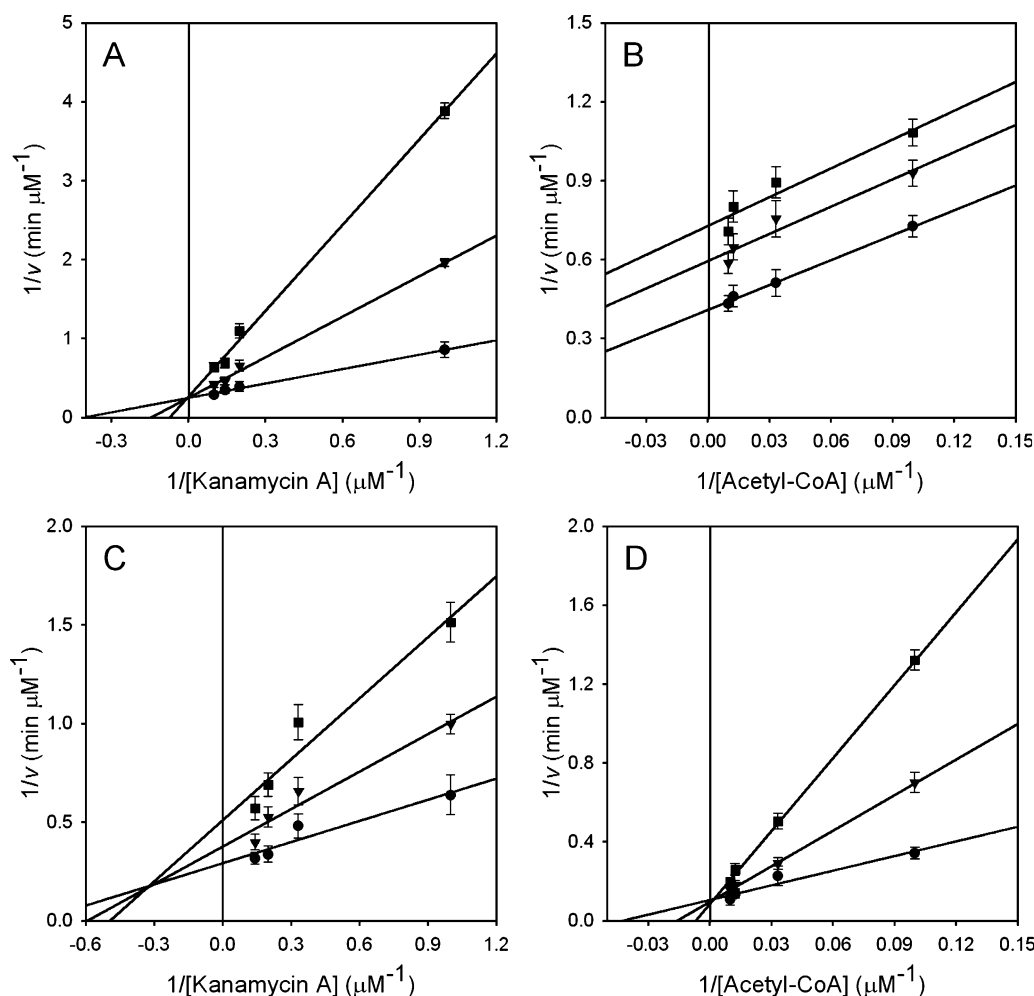
FIGURE 6: The inhibition patterns of dead-end inhibitors for the AAC(6′)-Ib′ domain. (A) Competitive inhibition by paromomycin (●, 2 μM; ▼, 5 μM; ■, 10 μM) with respect to kanamycin A (1−10 μM). (B) Uncompetitive inhibition by paromomycin (●, 25 μM; ▼, 50 μM; ■, 75 μM) with respect to acetyl-CoA (10−100 μM). (C) Noncompetitive/mixed inhibition by butyryl-CoA (●, 200 μM; ▼, 400 μM; ■, 800 μM) with respect to kanamycin A (1−7 μM). (D) Competitive inhibition by butyryl-CoA (●, 100 μM; ▼, 400 μM; ■, 1000 μM) with respect to acetyl-CoA (10−100 μM). Each data point was determined in triplicate, and the error bars indicate the data spread for each.

acetylated aminoglycoside and CoASH, in that order. On the other hand, ANT(3″)-Ii/AAC(6′)-IId has an ordered sequential Bi−Bi mechanism with aminoglycoside binding first followed by acetyl-CoA. Subsequent to the reaction, CoASH is released before the acetylated antibiotic. In contrast to the diversity of the kinetic mechanisms for APHs and ANTs, which include random ordered, ordered Bi−Bi, and Theorell−Chance mechanisms, AACs appear generally to have a random mechanism for their catalysis. The AAC-(3)-Ib domain of AAC(3)-Ib/AAC(6′)-Ib′, following a steady-state ordered Bi−Bi mechanism, gives added diversity to this class of enzymes.

The list of the over 50 known AAC enzymes testifies to their versatility as antibiotic resistance enzymes. The discoveries of the four bifunctional aminoglycoside-resistance enzymes represent a new twist in evolution of these enzymes. As antibiotics are used clinically, there are ample opportunities for the emergence of various mechanisms of resistance (45, 46). Once an antibiotic-resistance gene comes into existence, it undergoes mutation and selection to afford an enzyme that meets the survival needs of the organism. We have witnessed this evolutionary process in mutational

alterations of the genes that broaden the substrate profiles of these enzymes (for example, the cases of class A β-lactamases), or critical enzymes that maintain their physiological roles with less predisposition to inhibition by antibiotics (the cases of Gram-positive penicillin-binding proteins). The emergence of these bifunctional aminoglycoside-resistance enzymes is yet another level of sophistication. All three examples that have been studied—AAC(6′)/APH-(2″) (4−8), ANT(3)-Ii/AAC(6′)-IId (9), AAC(3)-Ib/AAC-(6′)-Ib′ (the present study)—reveal that the merger of the two genes results in bifunctional enzymes whose substrate profile was broadened. The cases of AAC(6′)/APH(2″) and ANT-(3″)-Ii/AAC(6′)-IId are somewhat intuitive, as two domains that catalyze distinct reactions merged to result in the large enzymes. The diversity of the reaction types gave rise to modification of aminoglycosides of diverse structural classes. Interestingly, this is also true for the subject of the present study, AAC(3)-Ib/AAC(6′)-Ib′. One might intuit that the advantage for the merger of the two AAC domains might be marginal, but the results of Table 1 argue to the contrary. Both domains turn over gentamicin and netilmicin, though with different catalytic parameters, hence there is some
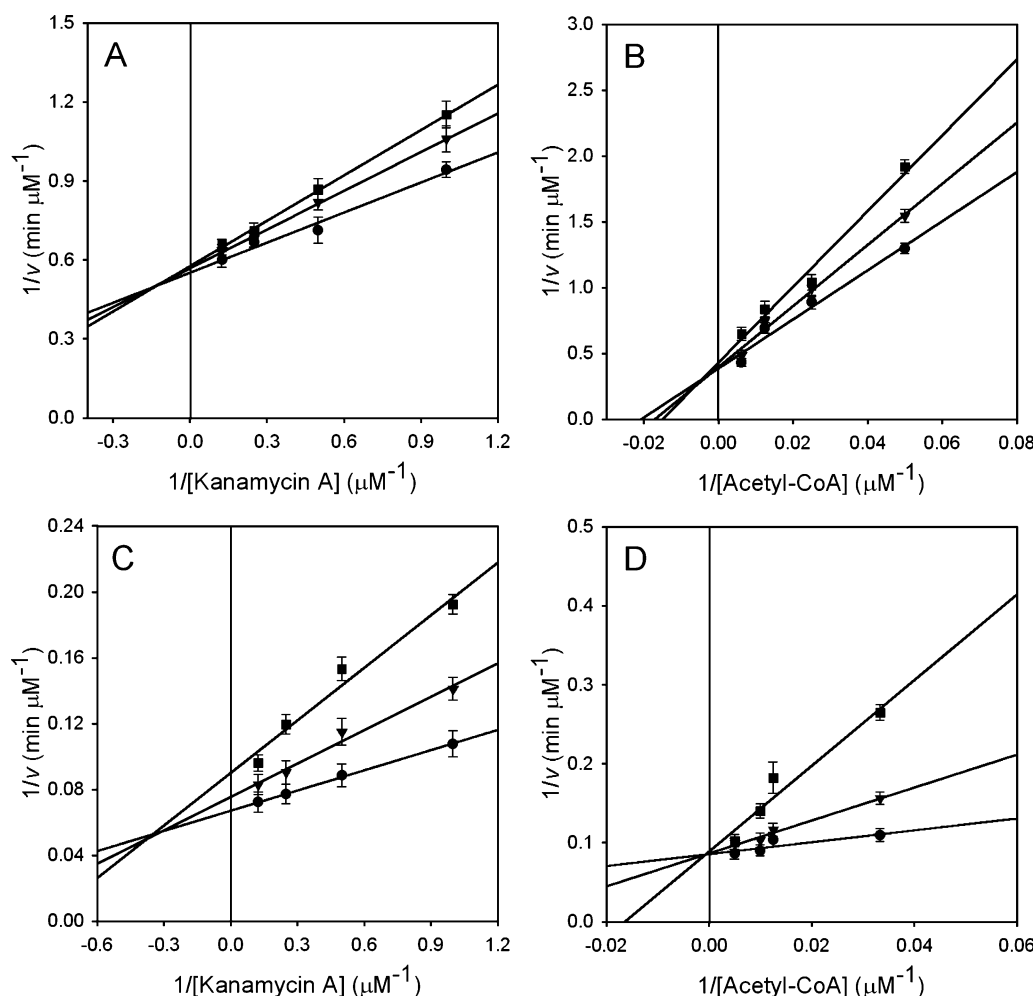
FIGURE 7: The inhibition patterns of the products for the AAC(6′)-Ib′ domain. (A) Noncompetitive/mixed inhibition by acetylated kanamycin A (AcKAN; ●, 5 μM; ▼, 10 μM; ■, 15 μM) with respect to kanamycin A (1−8 μM). (B) Noncompetitive/mixed inhibition by AcKAN (●, 50 μM; ▼, 70 μM; ■, 100 μM) with respect to acetyl-CoA (20−160 μM). (C) Noncompetitive/mixed inhibition by CoASH (●, 25 μM; ▼, 50 μM; ■, 100 μM) with respect to kanamycin A (1−8 μM). (D) Competitive inhibition by CoASH (●, 10 μM; ▼, 50 μM; ■, 200 μM) with respect to acetyl-CoA (30−200 μM).

Table 4: Solvent-Isotope Effects for the AAC(3)-Ib and AAC(6′)-Ib′ Domains

	AAC(3)-Ib				AAC(6′)-Ib′			
	K_m (μM)	k_{cat} (s^{-1})	k_{cat}^H/k_{cat}^D	$(k_{cat}/K_m)^H/(k_{cat}/K_m)^D$	K_m (μM)	k_{cat} (s^{-1})	k_{cat}^H/k_{cat}^D	$(k_{cat}/K_m)^H/(k_{cat}/K_m)^D$
	Gentamicin[a]				Kanamycin A[a]			
pH 6.5	3.1 ± 0.2	0.3 ± 0.01			nd	nd		
pD 6.5	2.3 ± 0.2	0.1 ± 0.01	3.0 ± 0.1	2.3 ± 0.3	nd	nd	nd	nd
pH 7.5	5.0 ± 0.8	0.3 ± 0.02			1.0 ± 0.1	2.4 ± 0.1		
pD 7.5	3.1 ± 0.2	0.1 ± 0.01	3.0 ± 0.2	1.9 ± 0.5	0.3 ± 0.1	0.9 ± 0.1	2.7 ± 0.3	0.8 ± 0.3
	Acetyl-CoA[c]				Acetyl-CoA[c]			
pH 6.5	3.0 ± 0.6	0.3 ± 0.02			nd	nd		
pD 6.5	2.2 ± 0.4	0.1 ± 0.01	3.0 ± 0.2	2.2 ± 0.4	nd	nd	nd	nd
pH 7.5	nd	nd			9.0 ± 4.0	1.0 ± 0.1		
pD 7.5	nd	nd	nd	nd	3.7 ± 0.5	0.5 ± 0.1	2.0 ± 0.4	0.8 ± 0.4

[a] Gentamicin and kanamycin A were used as variable substrates at a fixed concentration of acetyl-CoA (100 μM). [b] Not determined. [c] Solvent isotope effects were determined with varied concentrations of acetyl-CoA at the fixed gentamicin (100 μM) for AAC(3)-Ib and kanamycin A (5 μM) for AAC(6′)-Ib′.

overlap in their functions. Yet, the activity of the domain of broader substrate preference, AAC(6′)-Ib′, has been supplemented by turnover of fortimicin A by the AAC(3)-Ib domain. Fortimicin A has an atypical structure for an aminoglycoside, hence, considering the varieties of aminoglycoside structures that can serve as substrates for the bifunctional AAC(3)-Ib/AAC(6′)-Ib′, indeed the breadth of substrate preference has been broadened, to the advantage of the organism that harbors this enzyme.

ACKNOWLEDGMENT

A was a generous gift from Kyowa Hakko Kogyo Co., Ltd., Japan.

REFERENCES

1. Schwocho, L. R., Schaffner, C. P., Miller, G. H., Hare, R. S., and Shaw, K. J. (1995) Cloning and charaterization of a 3-*N*-aminoglycoside acetyltransferase gene, *aac(3)-Ib*, from *Pseudomonas aeruginosa, Antimicrob. Agents Chemother. 39*, 1790−1796.

2. Ahmed, A. M., Nakagawa, T., Arakawa, E., Ramamurthy, T., Shinoda, S., and Shimamoto, T. (2004) New aminoglycoside acetyltransferase gene, *aac(3)-Id*, in a class 1 integron from a multiresistant strain of *Vibrio fluvalis* isolated from an infant aged 6 months, *J. Antimicrob. Chemother. 53*, 947−951.

3. Levings, R. S., Partridge, S. R., Lightfoot, D., Hall, R. M., and Djordjevic, S. P. (2005) New integron-associated gene cassette encoding a 3-*N*-aminoglycoside acetyltransferase, *Antimicrob. Agents Chemother. 49*, 1238−1241.

4. Azucena, E., Grapsas, I., and Mobashery, S. (1997) Properties of a bifunctional bacterial antibiotic resistance enzyme that catalyzes ATP-dependent 2″-phosphorylation and acetyl-CoA-dependent 6′-acetylation of aminoglycosides, *J. Am. Chem. Soc. 119*, 2317−2318.

5. Daigle, D. M., Hughes, D. W., and Wright, G. D. (1999) Prodigious substrate specificity of AAC(6′)-APH(2″), an aminoglycoside antibiotic resistance determinant in enterococci and staphylococci, *Chem. Biol. 6*, 99−110.

6. Boehr, D. D., Lane, W. S., and Wright, G. D. (2001) Active site labeling of the gentamicin resistance enzyme AAC(6′)-APH(2″) by the lipid kinase inhibitor wortmannin, *Chem. Biol. 8*, 791−800.

7. Boehr, D. D., Jenkins, S. I., and Wright, G. D. (2003) The molecular basis of the expansive substrate specificity of the antibiotic resistance enzyme aminoglycoside acetyltransferase-6′-aminoglycoside phosphotransferase-2″−The role of Asp-99 as an active site base important for acetyl transfer, *J. Biol. Chem. 278*, 12873−12880.

8. Boehr, D. D., Daigle, D. M., and Wright, G. D. (2004) Domain-domain interactions in the aminoglycoside antibiotic-resistance enzyme AAC(6′)-APH(2″), *Biochemistry 43*, 9846−9855.

9. Kim, C., Hesek, D., Zajicek, J., Vakulenko, S. B., and Mobashery, S. (2006) Characterization of the bifunctional aminoglycoside-modifying enzyme ANT(3″)-Ii/AAC(6′)-IId from *Serratia marcescens, Biochemistry 45*, 8368−8377.

10. Dubois, V., Poirel, L., Marie, C., Arpin, C., Nordmann, P., and Quentin, C. (2002) Molecular characterization of a novel class 1 integron containing *bla*(GES−1) and a fused product of *aac3-Ib/aac6′-Ib′* gene cassettes in *Pseudomonas aeruginosa, Antimicrob. Agents Chemother. 46*, 638−645.

11. Tran Van Nhieu, G., and Collatz, E. (1987) Primary structure of an aminoglycoside 6′-*N*-acetyltransferase, AAC(6′)-4, fused *in vivo* with the signal peptide of the Tn3-encoded β-lactamase, *J. Bacteriol. 169*, 5708−5714.

12. Lambert, T., Ploy, M. C., and Courvalin, P. (1994) A spontaneous point mutation in the *aac(6′)-Ib′* gene results in altered substrate specificity of aminoglycoside 6′-*N*-acetyltransferase of a *Pseudomonas fluorescens* strain, *FEMS Microbiol. 115*, 297−304.

13. Casin, I., Bordon, F., Bertin, P., Coutrot, A., Podglajen, I., Brasseur, R., and Collatz, E. (1998) Aminoglycoside 6′-*N*-acetyltransferase variants of the Ib type with altered substrate profile in clinical isolates of *Enterobacter cloacae* and *Citrobater freundii, Antimicrob. Agents Chemother. 42*, 1211−1233.

14. Williams, J. W., and Northrop, D. B. (1978) Kinetic mechanisms of gentamicin acetyltransferase I: Antibiotic-dependent shift from rapid to nonrapid equilibrium random mechanisms, *J. Biol. Chem. 253*, 5902−5907.

15. Magalhaes, M. L. B., and Blanchard, J. S. (2005) The kinetic mechanism of AAC(3)-IV aminoglycoside acetyltransferase from *Escherichia coli, Biochemistry 44*, 16275−16283.

16. Kim, C., Haddad, J., Vakulenko, S. B., Meroueh, S. O., Wu, Y., Yan, H., and Mobashery, S. (2004) Fluorinated aminoglycosides and their mechanistic implication for aminoglycoside 3′-phosphotransferases from Gram-negative bacteria, *Biochemistry 43*, 2373−2383.

17. Bodenhausen, G., Freeman, R., Niedermeyer, R., and Turner, D. L. (1977) Double fourier transformation in high resolution NMR, *J. Magn. Reson. 26*, 133−164.

18. Bax, A., and Morris, G. A. (1981) An improved method for heteronuclear chemical shift correlation by two-dimensional NMR, *J. Magn. Reson. 42*, 501−505.

19. Bax, A., Griffey, R. H., and Hawkins, B. L. (1983) Correlation of proton and ^{15}N chemical shifts by multiple quantum NMR, *J. Magn. Reson. 55*, 301−315.

20. Bax, A., and Summers, M. F. (1986) ^{1}H and ^{13}C assignments from sensitivity-enhanced detection of heteronuclear multiple-bond connectivity by 2D multiple quantum NMR, *J. Am. Chem. Soc. 108*, 2093−2094.

21. Griesinger, C., Otting, G., Wuthrich, K., and Ernst, R. R. (1988) Clean TOCSY for ^{1}H spin system-identification in macromolecules, *J. Am. Chem. Soc. 110*, 7870−7872.

22. Wijmenga, S. S., Hallenga, K., and Hilbers, C. W. (1989) A three-dimensional heteronuclear multiple quantum coherence homonuclear Hartmann-Hahn experiment, *J. Magn. Reson. 84*, 634−642.

23. Wishart, D. S., Bigam, C. G., Yao, J., Abildgaard, F., Dyson, H. J., Oldfield, E., Markley, J. L., and Sykes, B. D. (1995) ^{1}H, ^{13}C and ^{15}N chemical shift referencing in biomolecular NMR, *J. Biomol. NMR 6*, 135−140.

24. Wright, G. D., and Ladak, P. (1997) Overexpression and characterization of the chromosomal aminoglycoside 6′-*N*-acetyltransferase from *Enterococcus faecium, Antimicrob. Agents Chemother. 41*, 956−960.

25. Hegde, S. S., Javid-Majd, F., and Blanchard, J. S. (2001) Overexpression and mechanistic analysis of chromosomally encoded aminoglycoside 2′-*N*-acetyltransferase (AAC(2′)-Ic) from *Mycobacterium tuberculosis, J. Biol. Chem. 276*, 45876−45881.

26. Lumry, R., Smith, E. L., and Glantz, R. R. (1951) Kinetics of carboxypeptidase action. I. Effect of various extrinsic factors on kinetic parameters, *J. Am. Chem. Soc. 73*, 4330−4340.

27. Schowen, K. B., and Schowen, R. L. (1982) Solvent isotope effects on enzyme systems, *Methods Enzymol. 87*, 551−606.

28. Chen-Goodspeed, M., Vanhooke, J. L., Holden, H. M., and Raushel, F. M. (1999) Kinetic mechanism of kanamycin nucleotidyltransferase from *Staphylococcus aureus, Bioorg. Chem. 27*, 395−408.

29. Morrison, J. F. (2001) Enzyme activity: Reversible inhibition, *Encycl. Life Sci. 1*, 1−8.

30. Magnet, S., Lambert, T., Courvalin, P., and Blanchard, J. S. (2001) Kinetic and mutagenic characterization of the chromosomally encoded *Salmonella enterica* AAC(6′)-Iy aminoglycoside *N*-acetyltransferase, *Biochemistry 40*, 3700−3709.

31. Hamano, Y., Hoshino, Y., Nakamori, S., and Takagi, H. (2004) Overexpression and characterization of an aminglycoside 6′-*N*-acetyltransferase with broad specificity from and ε-poly-L-lysine producer, *Streptomyces albulus* IFO14147, *J. Biochem. 136*, 517−524.

32. Wright, G. D., Berghuis, A. M., and Mobashery, S. (1998) Aminoglycoside antibiotics. Structures, functions, and resistance, *Adv. Exp. Med. Biol. 456*, 27−69.

33. Mingeot-Leclercq, M. P., Glupczynski, Y., and Tulkens, P. M. (1999) Aminoglycosides: Activity and resistance, *Antimicrob. Agents Chemother. 43*, 727−737.

34. Vakulenko, S. B., and Mobashery, S. (2003) Versatility of aminoglycosides and prospects for their future, *Clin. Microbiol. Rev. 16*, 430−450.

35. Martel, A., Masson, M., Moreau, N., and Le Goffic, F. (1983) Kinetic studies of aminoglycoside acetyltransferase and phosphotransferase from *Staphylococcus aureus* RPAL: Relation ship between the two activities, *Eur. J. Biochem. 133*, 515−521.

36. Radika, K., and Northrop, D. B. (1984) The kinetic mechanism of kanamycin acetyltransferase derived from the use of alternative antibiotics and coenzymes, *J. Biol. Chem. 259*, 12543−12546.

37. Gates, C. A., and Northrop, D. B. (1988) Alternative substrate and inhibition-kinetics of aminoglycoside nucleotidyltransferase-2″-I in support of a Theorell−Chance kinetic mechanism, *Biochemistry 27*, 3826−3833.

38. Siregar, J. J., Miroshnikov, K., and Mobashery, S. (1995) Purification, characterization, and investigation of the mechanism of aminoglycoside 3′-phosphotransferase type Ia, *Biochemistry 34*, 12681−12688.

39. McKay, G. A., and Wright, G. D. (1995) Kinetic mechanism of aminoglycoside phosphotransferase type IIIA−Evidence for a Theorell−Chance mechanism, *J. Biol. Chem. 270*, 24686−24692.

40. Azucena, E., and Mobashery, S. (2001) Aminoglycoside-modifying enzymes: mechanisms of catalytic processes and inhibition, *Drug Resist. Updates 4*, 106−117.

41. Draker, K. A., Northrop, D. B., and Wright, G. D. (2003) Kinetic mechanism of the GCN5-related chromosomal aminoglycoside acetyltransferase AAC(6′)-Ii from *Enterococcus faecium*, *Biochemistry 42*, 6565−6574.

42. Jana, S., and Deb, J. K. (2005) Kinetic mechanism of streptomycin adenylyltransferase from a recombinant *Escherichia coli*, *Biotechnol. Lett. 27*, 519−524.

43. Magnet, S., and Blanchard, J. S. (2005) Molecular insights into aminoglycoside action and resistance, *Chem. Rev. 105*, 477−497.

44. Rudolph, F. B. (1979) Product inhibition and abortive complex formation, *Methods Enzymol. 63*, 411−437.

45. Mobashery, S., and Azucena, E. (2002) Bacterial antibiotic resistance, *Encycl. Life Sci. 2*, 472−477.

46. Walsh, C. (2003) Where will new antibiotics come from?, *Nat. Rev. Microbiol. 1*, 65−70.